Studies of Water-Aluminum Scrap Reaction Kinetics in Two Steps and Efficiency of the Green Hydrogen Production

Ansis Mezulis[1], Christiaan Richter[2], Peteris Lesnicenoks[1], Ainars Knoks[1], Sarunas Varnagiris[3], Marius Urbanovicius[3], Darius Milcius[3], Janis Kleperis[1,*]

[1] Institute of Solid State Physics University of Latvia, Riga, Latvia; ansis.mezulis@cfi.lu.lv; peterisl@cfi.lu.lv; ainars.knoks@cfi.lu.lv; janis.kleperis@cfi.lu.lv;
[2] Faculty of Industrial Engineering, Mechanical Engineering and Computer Science, University of Iceland, Reykjavik, Iceland; cpr@hi.is;
[3] Center for Hydrogen Energy Technologies, Lithuanian Energy Institute, 3 Breslaujos, 44403 Kaunas; Lithuania; sarunas.varnagiris@lei.lt; marius.urbonavicius@lei.lt; darius.milcius@lei.lt;
* Correspondence: janis.kleperis@cfi.lu.lv

Abstract: The present work aims to explain the aluminum hydrolysis reaction kinetics based on properly chosen theoretical model with machined aluminum waste chips and alkali solutions up to 1M as a promoter, and to estimate overall reaction profit. In order to obtain results of better accuracy, we work with flat Al waste chips because a flat surface is preferable to maximally increase the time for created hydrogen bubbles to reach the critical gas pressure. At describing the reaction kinetics, flat shape allows using a planar one-dimensional shrinking core model instead of much complicated polydisperse spheric shrinking core model. We analyze the surface chemical reaction and mass transfer rate steps to obtain the first order rate constant for surface reaction and the diffusion coefficient of aqueous reactant in the byproduct layer, respectively. With our reactor we achieved H_2 yield of 1145 mL per 1 g Al with 1M NaOH, which is 92% of the theoretical maximum. At estimation of the profit, we pay much attention to the loss of alkaline and find a crucial dependence on its price. Nevertheless, in terms of consumed and originated materials for sale, conversion of the aluminum waste material into green hydrogen by properly chosen reaction parameters has a positive profit even by consuming alkali of chemical grade.

Keywords: aluminum waste; aluminum hydrolysis; alkali promoter; reaction rate; hydrogen production efficiency

1. Introduction

With the world primary aluminum production of 65 million metric tons in 2020, a worldwide issue of the residual aluminum waste from the industry is not resolved. Due to the content of domestic waste and amount of aluminous residual by-products, produced by the primary and secondary Al industry, aluminum can be found in a landfill in substantial quantities. In general, the byproduct of the aluminum recycling industry and the Bayer process is known as aluminum "dross". As in most regions Al dross is not classified as a hazardous waste material, it can be stored in landfill without any pretreatment. Nevertheless, Al rich waste in landfill may cause serious hazards. Aluminum, stored in landfill, after a period of time may come into contact with a kind of water source, including landfill leachate with pH < 7. Aqueous liquids, especially with pH < 7, are about to react with landfilled aluminum. As a result, pockets of concentrated hydrogen appear and their growing gaseous pressure in the landfill poses a risk of combustion. Subsurface landfill fires can be rather dangerous and destructive to a landfill system because they are hard to detect and visible smoke may not arise. Monitoring and control of the potentially hazardous wastes demand a lot of money that can be assigned to research and development of effective methods to deal with aluminous dross [1,2].

Findings and reported results of various studies on dealing with aluminum waste are always dependent on the region in with R&D work is carried on. One of the pioneering authors on this subject, Susana Silva Martinez et al. from Mexico, in 2005 reported hydrogen gas yield of 0.049 moles from each gram of aluminum waste cans with 2M NaOH promoter [3], being decent 88% of maximum yield from a pure aluminum. Hiraki and Akiyama from Japan in 2009 developed a system by which gaining energy of aluminum waste containing down to 15% Al is still cost effective [4]. Instead of using chemical promoters (hydroxides, oxides, salts), Ref. [5] deals with ball milling as a pre-treatment and proceeding the reaction in hot water. In Ref. [6] the difference between Al dross obtained from an aluminum recycling facility (RD), and Al dross directed to landfill is studied. The

Preprints (www.preprints.org) | NOT PEER-REVIEWED | Posted: 17 April 2023 doi:10.20944/preprints202304.0428.v1

authors report that with NaOH as the promoter, the RD and LD samples generated 0.50 and 0.15 liters of H_2 per 1g of Al. The maximum flow rates are measured as 2 L/min and 0.8 L/min, respectively. The authors claim that in a large scale this process can be cost-effective, moreover, the formation of bayerite and gibbsite has additional market value.

From the hydrogen production concept, obtaining H_2 by the reaction of certain metals with water has been a subject to investigate for many years. Among the number of metals that, at certain circumstances, can react with aqueous solutions to produce hydrogen, aluminum and its alloys are forwarded as the most suitable materials for the development of hydrogen production in future [7]. Aluminum can be transported and stored in a much simpler, safer and cheaper way than its end-product hydrogen. Comparing with the chemical rival sodium borohydride, aluminum is much less expensive and stable under normal conditions. The price of aluminum powder is more than 10 times lower than the price of sodium borohydride [7,8]. Some authors, e.g. Wang et. al. prove that produced H_2 by aluminum chemical reaction has a purity valid for a PEM fuel cell. A mini-type hydrogen generator from 25 wt.% Al alloy strips provides H_2 generation rate of about 38 mL/min at 0.01 mL/s dropping rate of sodium hydroxide solution [9]. Even though empirical evidence on the hydrogen production is substantial with controlled Al alloys and some types of processed Al waste, the reaction model may vary and is not completely clear. This work aims to explain the reaction mechanism based on properly chosen theoretical model and experimental findings with flat Al chips and alkali solutions up to 1M, and to estimate overall reaction profit.

2. Theoretical section

2.1. Aluminum surface and its reaction with water

Aluminum is known as a highly reactive chemical element that reacts with ambient oxygen to create a protective coating. A piece of aluminum, placed into solution, already has a coating of aluminum oxide or alumina, Al_2O_3. Aluminum oxide reacts with water at moderate temperature to produce a boehmite AlOOH layer. This is so called induction step:

$$Al_2O_3 + H_2O \rightarrow 2AlOOH \quad (1)$$

At the induction step the boehmite film grows, and the diffusion of OH^- ions through the AlOOH layer is considered. As a result, gaseous hydrogen bubbles appear at the Al:Al_2O_3 interface:

$$6AlOOH + 2Al \rightarrow 4Al_2O_3 + 3H_2\uparrow \quad (2)$$

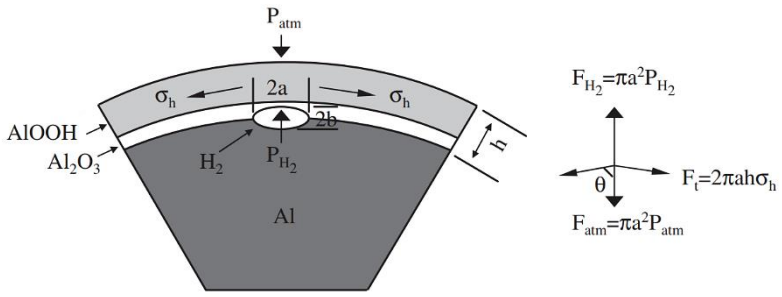

(a) (b)

Figure 1. An ellipsoidal H_2 bubble and the acting forces on it [10].

The thickness of surface passive oxide layer Al_2O_3 on each aluminum particle is several nanometers, being weakly dependent on the size of a spherical Al particle [11]. The time, needed for hydration of the oxide film,

Preprints (www.preprints.org) | NOT PEER-REVIEWED | Posted: 17 April 2023 doi:10.20944/preprints202304.0428.v1

has not a considerable difference for various Al powders. The difference in induction time mainly comes from the accumulation of H_2 molecules in gaseous bubbles to reach the critical gas pressure.

From the physical point of view, each gaseous H_2 bubble has its critical pressure that the hydrated oxide film can sustain, Figure 1a. When, by proceeding the chemical reaction, gas pressure in a H_2 bubble exceeds its critical threshold, the surface film on the Al particle locally breaks and the reaction of aluminum with water locally refreshes. From the vector diagram in Figure 1b, the critical gas pressure in a H_2 bubble, $P^*_{H_2}$, can be written as [12,13]:

$$P^*_{H_2} = P_{atm} + 2\frac{h\sigma_h cos\theta}{a}, \quad (3)$$

where P_{atm} is the environmental gas pressure, h – the thickness of the hydrated oxide film, a – the radius of a H_2 bubble, and σ_h is the tensile strength of the film. Theta, θ, is the critical angle between the stress vector $\overrightarrow{\sigma_h}$ and the normal axis to the film. Obviously, the time taken by the accumulation of H_2 quantity in the bubbles depends on their critical gas pressure. The critical gas pressure in the bubbles at the Al:Al_2O_3 interface must be less for smaller Al particles because smaller radius of a particle tends to reduce the total tolerable extension of a bubble on a surface. In other words, when the hydrogen gas pressure increases, the H_2 bubble expands, and for the small-sized Al particles the critical angle θ in Figure 1b has no further deviation from 90°. Noting that at normal conditions the first term, P_{atm}, is more than hundred times smaller than the second in Eq. (3), a small change of the critical angle θ leads to a large change of the critical gas pressure, $P^*_{H_2}$.

Regarding opposite consideration that a larger Al particle has a higher critical gas pressure and, due to that, larger-sized H_2 bubbles, a flat surface is preferable to maximally increase the time for the bubbles to reach the critical gas pressure. As increasing the induction time to perform the duration analysis ir advantageous for the present work, instead of spheric waste particles we prefer to examine chips, i.e., flat pieces of machined aluminum waste. At describing the reaction kinetics, it allows us using a planar one-dimensional shrinking core model instead of much complicated polydisperse spheric shrinking core model.

2.2. The role of the alkali promoter

All practicable Al reactions with water are intended to use a method to eliminate the protective layer of aluminum oxide, which hinders the reaction with water to proceed. Between different eliminators, a chemical promoter as sodium or potassium hydroxide works in a well-studied way. In the presence of sodium hydroxide as a promoter, aluminum oxide is being dissolved:

$$Al_2O_3 + 2NaOH + 3H_2O \rightarrow 2Na^+ + 2[Al(OH)_4]^- \quad (4)$$

As a result, exposed Al surface is able to react with water to form hydrogen:

$$2Al + 6H_2O \rightarrow 2Al(OH)_3 + 3H_2\uparrow \quad (5)$$

Created surface layer of aluminum hydroxide is being dissolved by sodium:

$$Al(OH)_3 + NaOH \rightarrow Na^+ + [Al(OH)_4]^- \quad (6)$$

Excluding dissociated ions, Eqs. (5, 6) can be composed as:

$$2Al\ (s) + 6H_2O + 2NaOH\ (aq) \rightarrow 2NaAl(OH)_4\ (aq) + 3H_2\uparrow \quad (7)$$

Summing up, even at room temperature aluminum and its alloys are dissolved in the alkaline environment, which results in H_2 production. Regeneration of sodium hydroxide occurs by decomposition of aqueous $NaAl(OH)_4$ and results in aluminum hydroxide residue:

$$NaAl(OH)_4\ (aq) \rightarrow NaOH\ (aq) + Al(OH)_3\ (s) \quad (8)$$

Preprints (www.preprints.org) | NOT PEER-REVIEWED | Posted: 17 April 2023 doi:10.20944/preprints202304.0428.v1

There are several parameters that affect this reaction chain: purity of aluminum material and its morphology, alkaline concentration, temperature, fresh alkaline feed rate.

2.3. Determining the activation energy

Considering the chemical reactions, the base parameter to estimate their occurrence is the activation energy of the reactant, i.e., the amount of energy needed for molecules or atoms to break existing chemical bonds. The activation energy, E_a, is defined by the Arrhenius equation:

$$k = Ae^{-\frac{E_a}{RT}}, \tag{9}$$

where k is the reaction rate constant, R – the universal gas constant, T - the absolute temperature, and A is frequency factor constant, value of which is rarely used. The reaction rate constant k here is assumed to be of "pure" chemical reaction, i.e., without any hindrances to maximum reaction rate. It is assumed that the first order rate constant for surface reaction k^* at sufficient stirring can be used as k. Usually E_a is derived from obtained reaction rate constants k at different temperatures. Applying the natural log to Eq. (9) yields:

$$\ln(k) = \ln(A) - \frac{E_a}{RT}, \tag{10}$$

obviously, with properly found values of k at various temperatures T, plotting ln(k) vs. 1/T displays a straight line, known as Arrhenius approximation. It's slope equals to -E_a/R, whereas the y-intercept equals to ln(A).

2.4. Reaction kinetics in two steps

According to the ideal-gas model, the hydrogen yield α ($0 < \alpha < 1$) can be written as:

$$\alpha(t) = \frac{p_{eff}V_{eff}}{n_0RT}, \tag{11}$$

where p_{eff} means the effective pressure (with subtracted initial gas pressure), V_{eff} – the effective volume (with subtracted volumes, occupied by liquid and powder), n_0 – theoretically calculated number of H_2 moles by reacting all of aluminum metal.

The aluminum-water reaction is a solid-liquid heterogeneous system. Usually, its reaction dynamics is described by the shrinking core model. A classical book [14] gives the formulas of the shrinking core for three geometries of reacting solid bodies: flat plates, cylinders and spheres. With the examined sample we choose the flat plates model, geometry of which is determined only by the half-thickness of the plate, r. Describing the reaction between a large number of small solid bodies and aqueous solution, two main reaction steps are considered.

2.4.1. Surface reaction rate step

In the first step the reaction rate is controlled by the surface chemical reaction, and the equation that describes shrinking of a flat solid plate at isothermal conditions is:

$$\frac{t}{\tau} = \alpha(t), \tag{12}$$

where t is the real time, and the characteristic time constant τ can be found from the equation:

$$\tau = \frac{r\rho_{Al}}{bk^*c_{alk}M_{Al}}, \tag{13}$$

where ρ_{Al} and M_{Al} are density and molar mass of the solid (aluminum), c_{alk} – the molar concentration of alkali aqueous promoter, and b is the stoichiometry coefficient in reaction between solid and liquid $d(n_{Al})=b\cdot d(n_{alk})$, being equal to 2/3 in examined reactions, Eq. (7). The first order rate constant for surface reaction k^* (mm/s) is the coefficient that is being determined by experimental data processing. In Ref. [15] it is suggested to take k^* as

Preprints (www.preprints.org) | NOT PEER-REVIEWED | Posted: 17 April 2023 doi:10.20944/preprints202304.0428.v1

a composition of the surface reaction rate constant k_s and the mass transfer constant in laminar boundary layers k_c:

$$\frac{1}{k^*} = \frac{1}{k_s} + \frac{1}{k_c}. \quad (14)$$

At sufficient stirring of aqueous alkali solution, $k_c >> k_s$ and $k^* \approx k_s$. In experiments one can choose intensity of the stirring and therefore to exclude the mass transfer constant k_c.

2.4.2. Mass transfer rate step

In the second step the reaction rate is mainly controlled by the mass transfer in the byproduct layer, and for a flat solid plate at isothermal conditions the corresponding equations are:

$$\frac{t}{\tau} = \alpha^2(t), \quad (15)$$

$$\tau = \frac{r^2 \rho_{Al}}{2bDc_{alk}M_{Al}}, \quad (16)$$

where D (mm²/s) is the diffusion coefficient of aqueous reactant in the byproduct layer. Likewise, the parameter k^* in the surface reaction rate step, D is the parameter to be determined by experimental data processing in the mass transfer rate step.

3. Materials and Methods

3.1. Experimental sample

Flat Al chips are a waste product from manufacturing aluminum constructions for insulating glass windows. We receive the chips, in average 0.2 mm thick, from Lithuanian company "Stiklita, JSC". Initial analysis of the chips is performed on the surface morphology by scanning electron microscope (SEM) Hitachi S3400 N and on the bulk elemental composition and elemental mapping by energy dispersive X-ray spectroscopy (EDS) Bruker Quad 5040. Additionally, crystal structure of initial Al material was examined by X-ray diffractometer (XRD) Brucker D8 using a Cu Kα radiation and Lynx Eye linear position detector at 2 theta angles in the range 20°-70°. The results of these analyses are compiled here in Figure 2. Alkalis pellets, NaOH and KOH, have purity of >99 %.

Preprints (www.preprints.org) | NOT PEER-REVIEWED | Posted: 17 April 2023 doi:10.20944/preprints202304.0428.v1

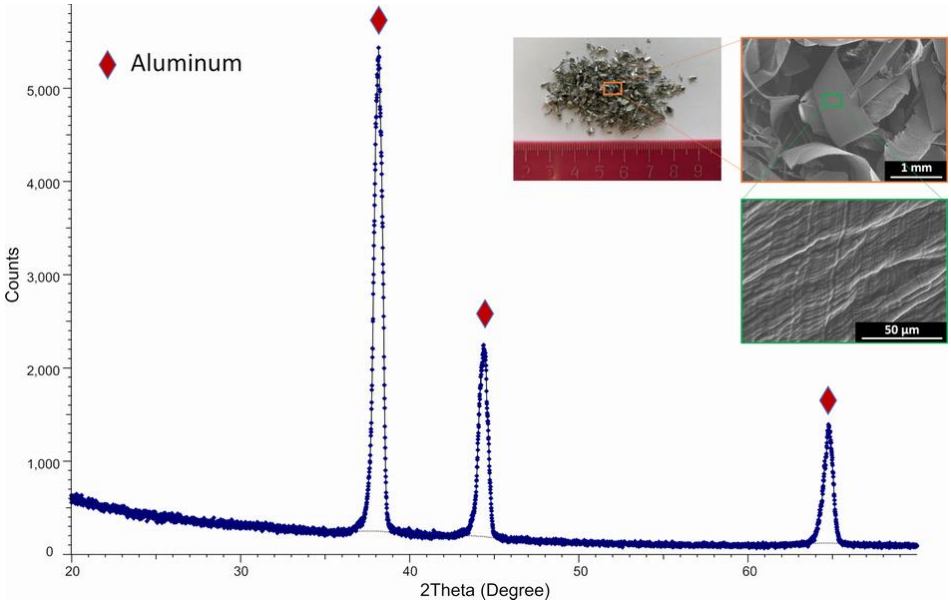

Figure 2. Initial waste Al chips: XRD graph; photo camera image; SEM images at different magnitude.

3.2. Experimental setup

To investigate aluminum hydrolysis, we use a custom-made laboratory stand shown in Figure 3. Before starting an experiment, we establish vacuum by the turbomolecular pump *6* of 10 Pa in all volumes designed for produced hydrogen spreading. Initial waste Al chips from the container *1* in a measured dose plunge into the reaction volume *3*. The magnetic stirrer is used to maintain sufficiently low mass transfer constant in laminar boundary layers solid-liquid. The water, needed for hydrolysis reaction, is deionized by the flow of argon bubbles. Produced hydrogen is purified by passing through water in the pre-volume *9* and spreads to the main volume, where its samples can be taken for the spectral analysis.

Since the whole volume occupied by the produced hydrogen is properly measured, we prefer to calculate the quantity of produced hydrogen by ideal-gas equation. For this aim we measure the pressure *10* and the temperature inside the volume *12*.

As we perform experiments with small quantities of Al chips (ca. 0.6 g) and low alkali concentrations (up to 1M), the reactor warms up due to exothermic behavior of the reaction approximately by five Celsius degrees, allowing to simplify the stand without building temperature stabilization of the reactor volume. All experiments have been carried out at constant laboratory temperature of 20°C. The temperature-dependent series, needed for Arrhenius approximation, have been performed previously by authors at the Center for Hydrogen Energy Technologies, Lithuanian Energy Institute.

Preprints (www.preprints.org) | NOT PEER-REVIEWED | Posted: 17 April 2023 doi:10.20944/preprints202304.0428.v1

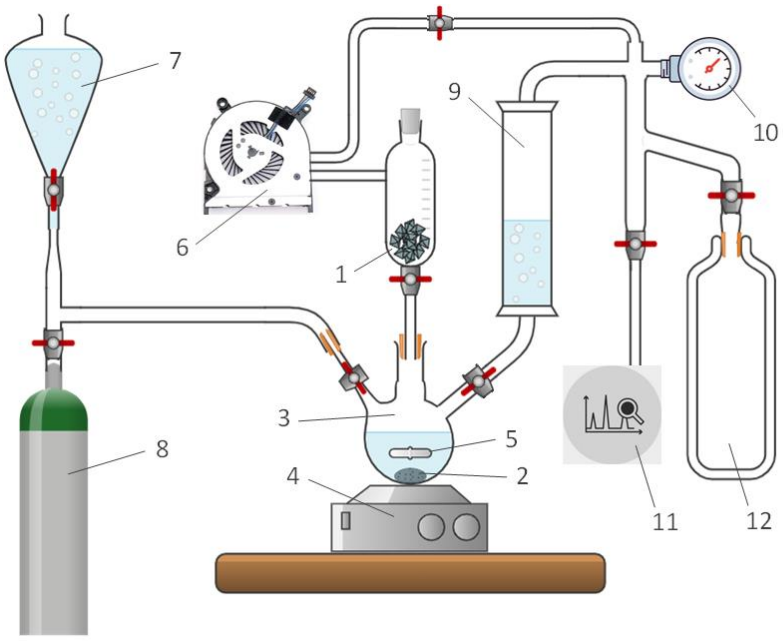

Figure 3. Experimental setup of the chemical reactor to produce hydrogen from aluminum. 1 – Al material (chips); 2 – $Al(OH)_3$ residue; 3 – reactor volume; 4 – magnetic stirrer; 5 – stirrer stick; 6 – turbomolecular pump; 7 – water deionizer; 8 – argon tank; 9 – gaseous hydrogen pre-volume; 10 – manometer; 11 – gas spectral analyzer; 12 – volume for produced hydrogen.

4. Results and Discussion

4.1. Stirring adjustment at the surface reaction rate step

Experiments, performed with 0.6 g Al chips in 50 ml alkali solution are assumed to run with excess alkaline. It means, at the surface chemical reaction step a sufficient stirring must provide a fresh surface contact between solid aluminum and alkali ions. In that case the maximum hydrogen production rate, mL/s, must be proportional to the alkali molar concentration. In our 100 mL reactor the stirring with magnetic field driven rotating stick works really efficiently; 300 rpm is enough to achieve a good linearity, as shown in Figure 4.

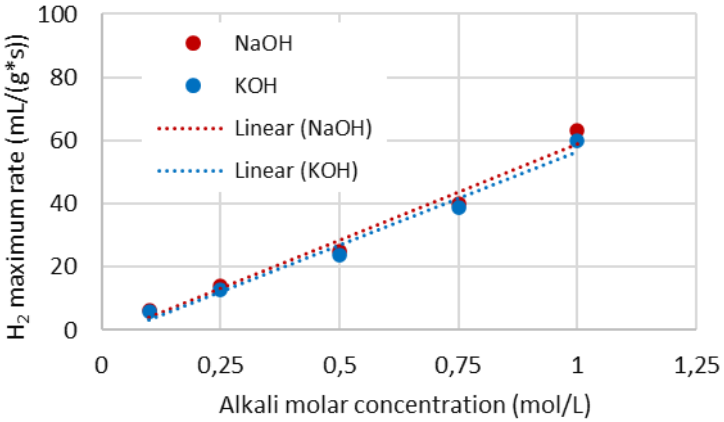

Figure 4. Stirring adjustment by reaching linearity.

4.2. Activation energy

The second step of our experimental work is determination of the activation energy from temperature-dependent series. In general, the activation energy is a property of examined solid material and should be independent from its flat plane thickness and alkali concentration. In Ref. [16] authors report a very slight

Preprints (www.preprints.org) | NOT PEER-REVIEWED | Posted: 17 April 2023 doi:10.20944/preprints202304.0428.v1

dependence of E_a on alkali concentration, which may be regarded to insufficient stirring. Reported difference of ca. 30% between a 0.02 mm thick foil and 0.5 mm thick plate is based on different structure and purity of aluminum material. As these effects are not the subject of present investigation; we have performed the tests to find a sufficient stirring rate and afterwards one proper temperature-dependent series with 0.24M NaOH. The Arrhenius plot built from obtained values of k is shown in Figure 5.

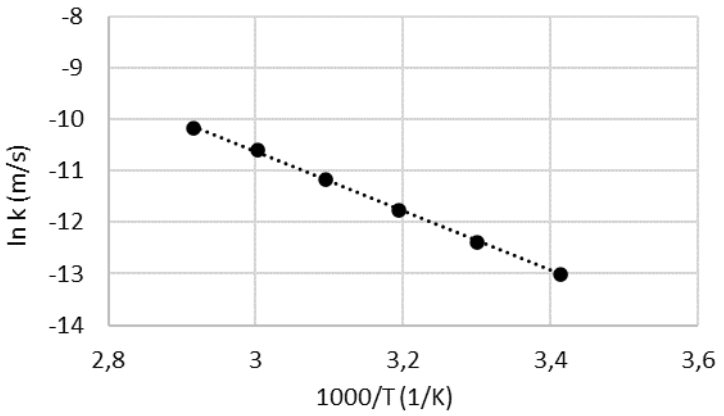

Figure 5. Arrhenius plot and its linear approximation with 0.24M NaOH solution.

The linear conformity in Fig. 5 is characterized by the R-squared value of 0.9992, being very good. From this series, the activation energy E_a is determined to be 48.1 kJ/mol. We can compare this value with given in Ref. [16], obtained by applying 1-2M NaOH alkali. Extrapolation of very small dependence on alkali molar concentration gives E_a = 40.9 kJ/mol with a 0.02 mm thick foil and 57.2 kJ/mol with 0.5 thick plates. Thus, the value of E_a of our 0.2 mm thick sample is somewhere in the middle, which is fully consistent regarding different material structures of the samples.

4.3. Normalized cumulative hydrogen yield

In Figure 4 we plot experimentally measured cumulative hydrogen yield, normalized to 1 g Al, vs. real time. One can see, with smaller alkali concentrations 0.1-0.5M the yield with NaOH a bit exceeds that with KOH, whereas with 0.75-1M it is the same.

Preprints (www.preprints.org) | NOT PEER-REVIEWED | Posted: 17 April 2023 doi:10.20944/preprints202304.0428.v1

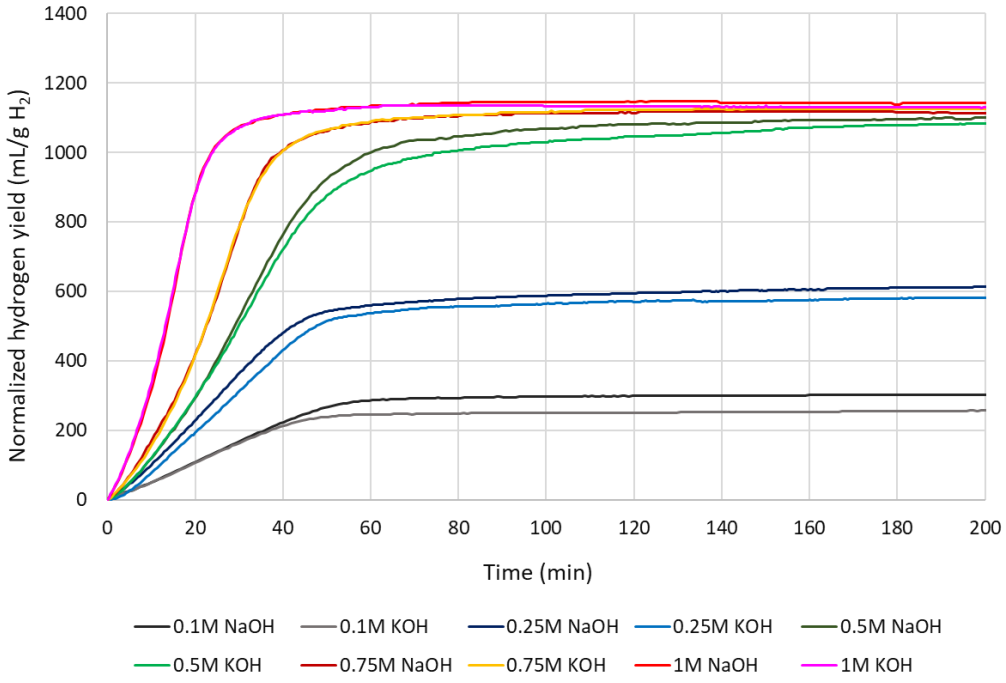

Figure 6. Experimentally measured cumulative H_2 yield.

Likewise in experiments with aluminum flakes in Ref. [17], we normalize further our cumulative yield levels to the highest one (1145 mL/g with 1M NaOH) in order to make the comparison, Figure 5. Despite the difference between pure alkalis NaOH, KOH and sodium aluminate $NaAlO_2$, the trend is very similar: more or less linearly the yield reaches ca. 95% level of its maximum at 0.5-0.6M of added aqueous promoter. The easiest explanation is that in the case of flat surface reaction, this value represents the threshold of alkali concentration to dissolve the surface layer of aluminum hydroxide sufficiently to expose a new Al surface, which reacts with water, Eq. (5).

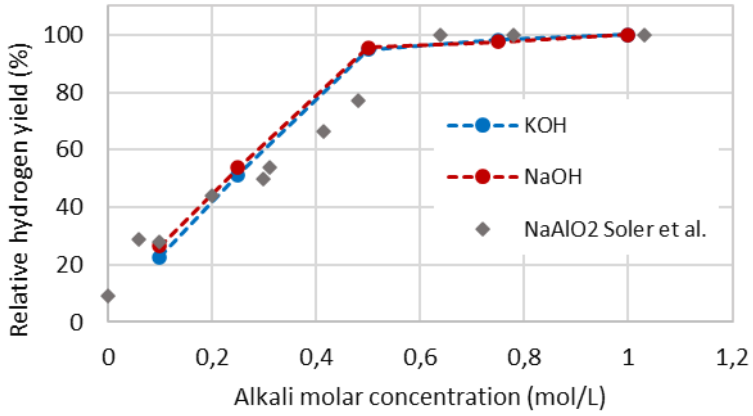

Figure 7. Comparison of normalized cumulative H_2 yields at different alkali concentrations.

A lot of authors perform the experiments with alkali concentrations above 1M [16,18-20]. As known, in the theory maximum H_2 yield of pure aluminum is 1245 mL/g, whereas we achieved with our experimental setup 1145 mL/g with 1M NaOH at moderate stirring. It is 92% of the maximum, and the deficit of 8% can be mainly regarded to not chemically pure aluminum. Thus, we consider the alkali concentration up to 1M as appropriate for the profit analysis.

Preprints (www.preprints.org) | NOT PEER-REVIEWED | Posted: 17 April 2023 doi:10.20944/preprints202304.0428.v1

4.4. Hydrogen production rate

Figure 8 displays experimentally taken H_2 production rate. Since H_2 cumulative yields with 1, 0.75 and 0.5M alkali are very close (Fig. 6), the areas below the production rate curves with corresponding alkali concentrations must be very close too. On the other hand, the corresponding three curves expose different slopes (Fig. 6), i.e., with a less alkali concentration the hydrogen production rate is distinctly lower. The mathematical solution of this problem, actually observed also in experiments, is a symmetrical stretching of the production rate curves in the time scale with lower alkali concentration. Indeed, the maximum hydrogen production rate with 1, 0.75 and 0.5M alkali is reached at 16, 27 and 35-th minute respectively. Notwithstanding, the production rate curves with alkali concentration less than 0.5M (0.1 and 0.25M) have smaller areas below and less distinct maximums.

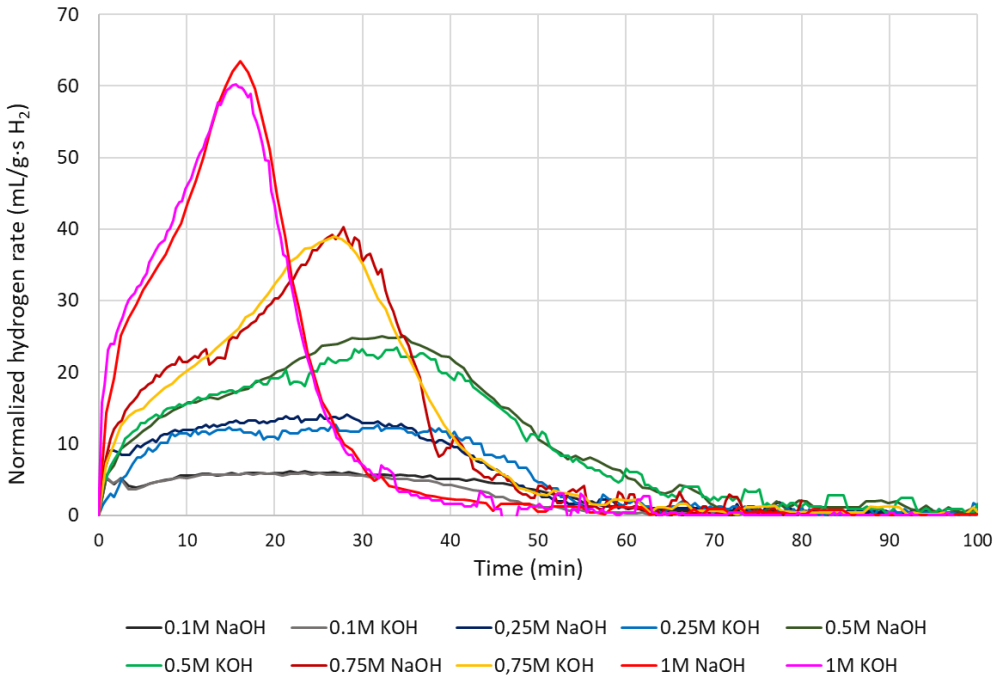

Figure 8. Experimentally measured H_2 production rate.

4.5. First order rate constant for surface reaction

Regarding Eqs. (12, 13), the best way to evaluate the first order rate constant k^* is to plot the hydrogen yield curves in coordinates: $x = \frac{M_{Al}}{\rho_{Al}} \cdot bc_{alk}t$ and $y = \alpha r_0$. The sloping of the best part of yield growth, measured by the linear trendline method, gives the value of k^* for each experimental conditions, depicted in Fig. 9. Regarding quantitative replicability of our chemical experiments, we estimate the error of k^* around ±1.5 μm/s, therefore we tend to take the first order rate constant as independent from alkali concentration at least up to 1M. This finding coincides with theoretical opinion, that at properly performed surface reaction step the reaction rate k^* is linearly proportional to c_{alk} [14].

Preprints (www.preprints.org) | NOT PEER-REVIEWED | Posted: 17 April 2023 doi:10.20944/preprints202304.0428.v1

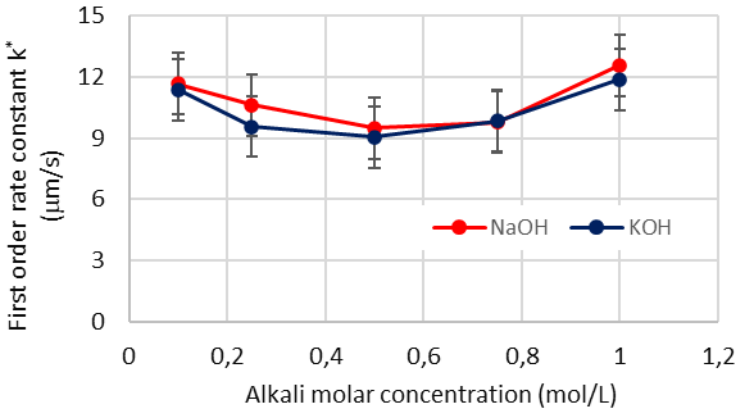

Figure 9. Evaluated first order rate constants k^* for surface reaction at different alkali concentrations.

Ref. [15] gives the values with powdered aluminum reagent (Kojundo Chemical Laboratory Co., Ltd.) having 99% mass purity and a particle size of 180–425 µm, with 0.5M NaOH of 1.97 µm/s at 20 °C and 22.8 µm/s at 40 °C. Since the temperature in our reactor is ca. 25 °C, value of 9.5 µm/s (Fig. 9) seems to be consistent. A precise comparison is not possible as the value is strongly influenced by both temperature and Al material and its characteristic size.

Noting the error bars, the difference between NaOH and KOH in Fig. 9 is not proven. Nevertheless, we point out that some authors have found NaOH a little more active than KOH. It can be explained by slightly different mechanisms of catalysis for each alkali. Ref. [16] reports that the activation energies for performed experiments are larger in the presence of KOH over NaOH. The activation energy E_a of corrosion is related to the exchange current density i_c: for slower corrosion E_a is larger and i_c is smaller, and vice-versa [21]. This allows the explanation that in open corrosion process the value of i_c in reaction with KOH is a bit less than that with NaOH.

4.6. Diffusion coefficient of aqueous reactant in the byproduct layer

In order to obtain the first order rate constant, in accordance with Eqs. (15, 16) we define new particular coordinates to evaluate the diffusion coefficient in the byproduct layer: $x = \frac{M_{Al}}{\rho_{Al}} \cdot bc_{alk}t$ and $y = \alpha^2 \frac{r_0^2}{2}$.

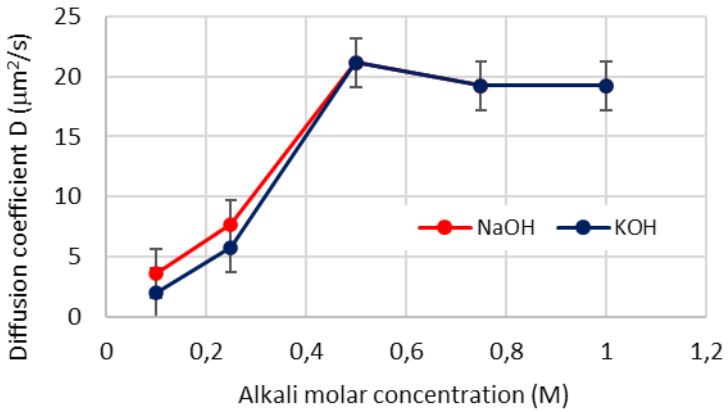

Figure 10. Evaluated second order rate constants D for mass transfer at different alkali concentrations.

Figure 10 displays evaluated values of the diffusion coefficient of aqueous reactant in the byproduct layer D. Based on restricted quantitative replicability of our experiments, we estimate the error of D around ±2 µm²/s. Noting this error, the diffusion coefficient D seems to be constant starting from 0.5M at the value of approx. 19 µm²/s, Fig. 10. Very low values of D with 0.1 and 0.25M can be explained by slow forming of H_2 bubbles up

Preprints (www.preprints.org) | NOT PEER-REVIEWED | Posted: 17 April 2023 doi:10.20944/preprints202304.0428.v1

to its critical pressure (Fig. 1) and, due to that, by low intensity of local breaking Al surface film to refresh the reaction with water. Likewise in Fig. 9, the difference between NaOH and KOH at 0.1 and 0.25M in Figure 10 cannot be proven.

4.7. Economic Analysis

4.7.1. Profit estimation of performed experiments

The hydrogen yield curves (Fig. 6) and analysis discussed above indicate that with NaOH or KOH concentrations starting from 0.5M the yield approaches its real maximum. Hence, in terms of the key criterion of optimizing yield, the conclusion is that any molarity of either NaOH or KOH ≥0.5M are potential candidates for the optimal economical production of hydrogen via hydrolysis.

Considering optimization of reaction conditions in terms of economics, the next criterion is the reaction rate. We see in Figure 6 that at 1M the reaction goes to completion in about 60 minutes, compared to 90 minutes at 0.75M and even up to 160 minutes at 0.5M. Hence, for a plant with a target hydrogen production rate, or equivalently a given waste Al throughput rate, the reactor volume must be increased by approximately 1.5 times if an operation opts for production at 0.75M rather than 1M. Although such a saving on CAPEX (reactor size) should certainly be taken into account in process economics, it is far from a magnitude that allows clear conclusions.

In our opinion, very few authors who give a simple profit estimation of aluminum hydrolysis process, pay attention to the loss of cycled alkali. Although NaOH is not consumed by the reaction chain, Eqs. (4-8), i.e., no NaOH would have to be replaced in the ideal case, XRF indicates that ca. 6-10 % of 6M NaOH ends up in cycled natrium hydroxide solution, even rinsed to neutral pH after removing from the reaction volume [22]. Having no detailed investigations on NaOH loss at different initial molarities, it seems to be sensibly to assume the relative loss proportional to the initial molarity, giving ca. 1.33% with 1M NaOH. At laboratory work alkali of the chemical grade is usually referred. A good price point of 50 wt.% NaOH solution in water of chemical grade can be found at Sigma-Aldrich (code 415413), served in 18 L drums. The same NaOH solution of technical grade, served in 200 L drums (680 lbs.) is seven times cheaper, see Table 1 [23].

Our simple profit estimation is made for NaOH promoter both of chemical and technical grade, and shown in Table 1. In North Europe there is no fixed price for machined waste aluminum chips; we use a value found in reports of 0.5 €/kg. Regarding the hydrogen yield, there is no sense to distinguish our real yield as 92% of the theoretical (stoichiometric) yield because we take the most frequent price point of European sales 6-8 €/kg, which makes uncertainty of 25% by itself [24]. In this profit estimation we account the price of gibbsite because the expenses of the calcination may depend on the grade of NaOH, being discussed below. As it is seen from Table 1, the difference in profit between applying NaOH of chemical or technical grade is crucial. If all prices and sales are well estimated, applying 1M NaOH of chemical grade leads even to negative profit.

Table 1. Profit estimation of aluminum hydrolysis with NaOH promoter of chemical and technical grade (per 1 kg H_2 yield).

Al chips 9 kg	**Green H_2 sale 1 kg**	**Gibbsite sale 26 kg**	**NaOH price 26.6 kg 50 wt.% (aq)**	**NaOH loss of 1.33% (with 1M NaOH)**	**Profit of Al hydrolysis process**
0.5 €/kg · 9 kg = 4.5 €	6 €	0.2 €/kg · 26 kg = 5.2 €	chemical: 547 €	7.3 €	- 0.6 €
			technical: 76 €	1.0 €	5.7 €

There is a dilemma of losing less NaOH vs. increasing the reaction time from 60 min to 90 min with choosing alkali concentration between 1M and 0.75M. Table 2 deals with calculated "over-profit" by shifting from 1M to

Preprints (www.preprints.org) | NOT PEER-REVIEWED | Posted: 17 April 2023 doi:10.20944/preprints202304.0428.v1

0.75M, related to the overtime of 1 hour. As expected, the difference in over-profit between chemical and technical grade of NaOH is huge, i.e., nine times.

Table 2. Over-profit estimation by shifting from 1M to 0.75M NaOH, related to 1 h overtime (per 1 kg H_2 yield).

NaOH price 26.6 kg 50 wt.% (aq)	NaOH loss of 1.33% (with 1M NaOH)	Profit of Al hydrolysis process with 1M	NaOH loss of 1% (with 0.75M NaOH)	Profit of Al hydrolysis process with 0.75M	"Over-profit" of decreased NaOH molarity vs. overtime
chemical: 547 €	7.3 €	- 0.6 €	5.5 €	1.2 €	3.6 €/h
technical: 76 €	1.0 €	5.7 €	0.76 €	5.9 €	0.4 €/h

4.7.2. Open problems of further treatment of aluminum hydroxide

To determine the most economical alkali hydroxide concentration for production, or to consider switching from the alkali hydroxides to $Ca(OH)_2$ [25,26], two related additional criteria have to be pointed out:

- Hydroxide salt make-up required between the runs;
- Impurity levels of chemical elements within the solid aluminum hydroxide $Al(OH)_3$ product and its general suitability for recycling/end-use.

The most viable known use of the solid $Al(OH)_3$ product is recycling it back to primary aluminum production. This could constitute "ideal recycling" as opposed to, for example, the "down-cycling" in which aluminum is being "sweetened" (diluted) by a significant amount of virgin aluminum from a smelter (20% to 96% depending on feedstock quality and target alloy) [27-29]. Other examples of the "down-cycling" are common plastic recycling and even the current state of the art of most aluminum scrap recycling where the impurity levels of chemical elements require that recycled.

In order to return the solid $Al(OH)_3$ product to aluminum smelters, the hydroxide needs to be converted to oxide or alumina, Al_2O_3. Ideal recycling would be enabled if the hydrolysis product does not incorporate, or entrain, more alkali metal or Ca than the smelter specification accepts. Aluminum smelters typically have accepted specifications on the surface areas (typically ca. 75 m^2/g) and impurity levels of alumina (e.g., ≤0.2 wt.% for elements like Na, K or Ca). Given an acceptably low impurity profile, aluminum hydroxide can be converted to alumina by calcination either as part of the recycling operation itself, or by shipping the solid $Al(OH)_3$ product to an existing bauxite processing facility. In the case of shipping the hydroxide from the hydrolysis recycler can be co-introduced with the ore early in the extraction process or directly co-mingled with derived gibbsite, γ-$Al(OH)_3$, by the Bayer process at the final calcination step. Generally, calcination in a large scale by now is very low efficient process in terms of energy. The thermodynamic minimum to treat 1 kg Al is only 0.1 kWh whereas publications report real energy use of 1.6 kWh [30]. In another event, gibbsite, being the dominant crystal phase of the aluminum hydroxide in ore and also the hydroxide precipitate formed within the Bayer process itself [31], would be the preferred phase since the widely used standard calcination conditions of the hydroxide reliably results in an alumina powder that meets the specific surface area and other specifications for the alumina feedstock of smelters. This is not a trivial consideration because the formation of the less common synthetic aluminum hydroxide phase bayerite, α-$Al(OH)_3$, and the undesirable incorporation of a sufficient amount of cations like Na^+ or Ca^{2+} to form XRD detectable amounts of species like sodium aluminate or kotoite as part of the solid hydrolysis product, has been frequently reported under standard hydrolysis conditions [15,25,26]. The formation of bayerite is less of a problem than the challenge posed by the impurities. Bayerite often naturally transforms to gibbsite, likely because it is entropically favored, or one could probably research and demonstrate calcination conditions for bayerite not too distinct from those for gibbsite where the resulting alumina meets the surface area specifications of smelters [32]. However, the impurities will likely play a key role in the morphology and surface area upon calcination; it is known that even small amounts

 doi:10.20944/preprints202304.0428.v1

of impurities like fluoride, chloride and alkali cations or alkali oxides (that can generally be reduced by careful product washing), or larger amounts of impurities like carbonate (that is hard to remove fully by washing once resent) can play a critical role in determining the phase and morphology, including pore structure and surface area of the alumina powder produced from hydroxide by a given calcination protocol [32]. Additional difficulties in gibbsite calcination to alumina after applying NaOH of technical grade are not surely found in literature.

5. Conclusions

The activation energy for out flat Al chips is determined to be 48.1 kJ/mol that consists with referred E_a = 40.9 kJ/mol with a 0.02 mm thick foil and 57.2 kJ/mol with 0.5 thick plates. The cumulative hydrogen yield , achieved in our experiments, reaches 1145 mL per 1 g Al with 1M NaOH at moderate stirring, which is 92% of theoretical (stoichiometric) H_2 yield of pure aluminum, 1245 mL/g. Evaluated the first order rate constant of chemical reaction k^* is rather independent from the alkali concentration up to 1M. Notwithstanding, the diffusion coefficient of aqueous reactant in the byproduct layer D seems to be constant starting from 0.5M. Determined values of k^* and D have sufficient accuracy to be used in mathematical simulation of chemical and physical processes for the present type of Al chips. Although NaOH shows a bit more activity as the promoter than KOH, noting the error bars, that difference is not proven. Profit estimation of aluminum hydrolysis reviles a crucial difference between applying NaOH of chemical or technical grade, if attention is paid to the loss of cycled alkali. It seems possible to reduce the expenses due to alkali by applying it at a lower concentration, down to 0.75M, allowing extra time for reaction to proceed.

6. Acknowledgement

This research is funded by the Baltic Research Programme project No. EEA-RESEARCH-92 , EEA Grant No. EEZ/BPP/VIAA/2021/5

7. References

[1] G. V. Calder and T. D. Stark, “Aluminum reactions and problems in municipal solid waste landfills,” *Practice Periodical of Hazardous, Toxic, and Radioactive Waste Management*, vol. 14, no. 4, pp. 258–265, Sep. 2010, doi: 10.1061/(ASCE)HZ.1944-8376.0000045.

[2] “Primary Aluminium Production - International Aluminium Institute.” https://international-aluminium.org/statistics/primary-aluminium-production/ (accessed Jan. 29, 2023).

[3] L. Soler, J. Macanás, M. Muñoz, and J. Casado, “Aluminum and aluminum alloys as sources of hydrogen for fuel cell applications,” *J Power Sources*, vol. 169, no. 1, pp. 144–149, Jun. 2007, doi: 10.1016/J.JPOWSOUR.2007.01.080.

[4] T. Hiraki and T. Akiyama, “Exergetic life cycle assessment of new waste aluminium treatment system with co-production of pressurized hydrogen and aluminium hydroxide,” *Int J Hydrogen Energy*, vol. 34, no. 1, pp. 153–161, Jan. 2009, doi: 10.1016/J.IJHYDENE.2008.09.073.

[5] S. S. Razavi-Tousi and J. A. Szpunar, “Mechanism of Corrosion of Activated Aluminum Particles by Hot Water,” *Electrochim Acta*, vol. 127, pp. 95–105, May 2014, doi: 10.1016/J.ELECTACTA.2014.02.024.

[6] E. Elsarrag, A. Elhoweris, and Y. Alhorr, “The production of hydrogen as an alternative energy carrier from aluminium waste,” *Energy Sustain Soc*, vol. 7, no. 1, pp. 1–14, Dec. 2017, doi: 10.1186/S13705-017-0110-7/TABLES/2.

[7] J. Xuan, M. K. H. Leung, D. Y. C. Leung, and M. Ni, "A review of biomass-derived fuel processors for fuel cell systems," *Renewable and Sustainable Energy Reviews*, vol. 13, no. 6–7, pp. 1301–1313, 2009, Accessed: Jan. 29, 2023. [Online]. Available: https://ideas.repec.org/a/eee/rensus/v13y2009i6-7p1301-1313.html

[8] S. C. Amendola *et al.*, "A Safe, portable, hydrogen gas generator using aqueous borohydride solution and Ru catalyst," *Int J Hydrogen Energy*, vol. 25, no. 10, pp. 969–975, Oct. 2000, doi: 10.1016/S0360-3199(00)00021-5.

[9] E. D. , S. P. F. , D. C. Y. , W. X. R. Wanga, "A mini-type hydrogen generator from aluminum for proton exchange membrane fuel cells," *J Power Sources*, vol. 181, pp. 144–148, 2008.

[10] W. Z. Gai, W. H. Liu, Z. Y. Deng, and J. G. Zhou, "Reaction of Al powder with water for hydrogen generation under ambient condition," *Int J Hydrogen Energy*, vol. 37, no. 17, pp. 13132–13140, Sep. 2012, doi: 10.1016/J.IJHYDENE.2012.04.025.

[11] B. C. Bunker *et al.*, "Hydration of Passive Oxide Films on Aluminum," *Journal of Physical Chemistry B*, vol. 106, no. 18, pp. 4705–4713, May 2002, doi: 10.1021/JP013246E.

[12] Z. Y. Deng, J. M. F. Ferreira, Y. Tanaka, and J. Ye, "Physicochemical Mechanism for the Continuous Reaction of γ-Al2O3-Modified Aluminum Powder with Water," *Journal of the American Ceramic Society*, vol. 90, no. 5, pp. 1521–1526, May 2007, doi: 10.1111/J.1551-2916.2007.01546.X.

[13] Z. Y. Deng, J. M. F. Ferreira, and Y. Sakka, "Hydrogen-generation materials for portable applications," *Journal of the American Ceramic Society*, vol. 91, no. 12, pp. 3825–3834, Dec. 2008, doi: 10.1111/J.1551-2916.2008.02800.X.

[14] O. Levenspiel, "Chemical Reaction Engineering, 3rd Edition | Wiley," *New York*, p. 704, 1998, Accessed: Jan. 29, 2023. [Online]. Available: https://www.wiley.com/en-us/Chemical+Reaction+Engineering%2C+3rd+Edition-p-9780471254249

[15] T. Hiraki, M. Takeuchi, M. Hisa, and T. Akiyama, "Hydrogen production from waste aluminum at different temperatures, with LCA," *Mater Trans*, vol. 46, no. 5, pp. 1052–1057, May 2005, doi: 10.2320/MATERTRANS.46.1052.

[16] C. B. Porciúncula, N. R. Marcilio, I. C. Tessaro, and M. Gerchmann, "Production of hydrogen in the reaction between aluminum and water in the presence of NaOH and KOH," *Brazilian Journal of Chemical Engineering*, vol. 29, no. 2, pp. 337–348, Apr. 2012, doi: 10.1590/S0104-66322012000200014.

[17] L. Soler, A. M. Candela, J. Macanás, M. Muñoz, and J. Casado, "In situ generation of hydrogen from water by aluminum corrosion in solutions of sodium aluminate," *J Power Sources*, vol. 192, no. 1, pp. 21–26, Jul. 2009, doi: 10.1016/J.JPOWSOUR.2008.11.009.

[18] S. S. Martínez, W. L. Benítes, A. A. Á. Gallegos, and P. J. Sebastián, "Recycling of aluminum to produce green energy," *Solar Energy Materials and Solar Cells*, vol. 88, no. 2, pp. 237–243, Jul. 2005, doi: 10.1016/J.SOLMAT.2004.09.022.

[19] "(1) (PDF) Design of Hydrogen Generator for On-Board Hydrogen Generation from Waste Aluminum Chips." https://www.researchgate.net/publication/303382386_Design_of_Hydrogen_Generator_for_On-Board_Hydrogen_Generation_from_Waste_Aluminum_Chips (accessed Jan. 29, 2023).

 doi:10.20944/preprints202304.0428.v1

[20] "(1) Analysis of Valorization Process of Aluminum Breakage Scraps to Obtain Green Hydrogen | Request PDF." https://www.researchgate.net/publication/350299739_Analysis_of_Valorization_Process_of_Aluminum_Breakage_Scraps_to_Obtain_Green_Hydrogen (accessed Jan. 29, 2023).

[21] C. M. A. Brett, A. N. A. Maria, and O. Brett, "Principles , Methods , and Applications," *Electrochemistry*, vol. 67, no. 2, p. 444, 1993, Accessed: Jan. 29, 2023. [Online]. Available: http://www.getcited.org/pub/102998784

[22] "AlEnCycles - Aluminium-Redox-Cycles for the Production of Heat and Electricity for Buildings based on Renewable Energies | Zenodo." https://zenodo.org/record/6393255#.ZBjQkMJBy70 (accessed Mar. 20, 2023).

[23] "Sodium Hydroxide / Caustic Soda Supplier & Distributor | Univar Solutions | Univar Solutions." https://www.univarsolutions.com/product-categories/essential-chemicals-ingredients/liquid-caustic-soda?hasprice=cspweb (accessed Mar. 20, 2023).

[24] "Hydrogen cost and sales prices | H2Valleys." https://h2v.eu/analysis/statistics/financing/hydrogen-cost-and-sales-prices (accessed Mar. 20, 2023).

[25] W. Z. Gai, L. Y. Wang, M. Y. Lu, and Z. Y. Deng, "Effect of low concentration hydroxides on Al hydrolysis for hydrogen production," *Energy*, vol. 268, p. 126731, Apr. 2023, doi: 10.1016/J.ENERGY.2023.126731.

[26] S. Kanehira *et al.*, "Controllable hydrogen release via aluminum powder corrosion in calcium hydroxide solutions," *Journal of Asian Ceramic Societies*, vol. 1, no. 3, pp. 296–303, Sep. 2013, doi: 10.1016/J.JASCER.2013.08.001.

[27] Y. Zhu and D. R. Cooper, "An Optimal Reverse Material Supply Chain for U.S. Aluminum Scrap," *Procedia CIRP*, vol. 80, pp. 677–682, Jan. 2019, doi: 10.1016/J.PROCIR.2019.01.065.

[28] V. K. Soo, J. R. Peeters, P. Compston, M. Doolan, and J. R. Duflou, "Economic and Environmental Evaluation of Aluminium Recycling based on a Belgian Case Study," *Procedia Manuf*, vol. 33, pp. 639–646, Jan. 2019, doi: 10.1016/J.PROMFG.2019.04.080.

[29] R. Modaresi and D. B. Müller, "The role of automobiles for the future of aluminum recycling," *Environ Sci Technol*, vol. 46, no. 16, pp. 8587–8594, Aug. 2012, doi: 10.1021/ES300648W/SUPPL_FILE/ES300648W_SI_001.PDF.

[30] M. Y. Haller, D. Amstad, M. Dudita, A. Englert, and A. Häberle, "Combined heat and power production based on renewable aluminium-water reaction," *Renew Energy*, vol. 174, pp. 879–893, Aug. 2021, doi: 10.1016/J.RENENE.2021.04.104.

[31] J. D. Gale, A. L. Rohl, V. Milman, and M. C. Warren, "An ab Initio Study of the Structure and Properties of Aluminum Hydroxide: Gibbsite and Bayerite," *Journal of Physical Chemistry B*, vol. 105, no. 42, pp. 10236–10242, Oct. 2001, doi: 10.1021/JP011795E.

[32] "Oxides and hydroxides of aluminum | WorldCat.org." https://www.worldcat.org/title/oxides-and-hydroxides-of-aluminum/oclc/18997314 (accessed Mar. 18, 2023).